

Journal Pre-proof

Active Bio-Based Packaging for Fresh-Cut Melon: Antimicrobial Efficacy and Zinc Migration of Nanocellulose/ZnO Nanocomposite Films

Ana Rita Mendes, Francisco A.G. Soares Silva, Cristina Mena, Fátima Silva, Cristina L.M. Silva, Paula Teixeira, Fátima Poças



PII: S0956-7135(26)00264-1

DOI: <https://doi.org/10.1016/j.foodcont.2026.112219>

Reference: JFCO 112219

To appear in: *Food Control*

Received Date: 29 January 2026

Revised Date: 28 March 2026

Accepted Date: 14 April 2026

Please cite this article as: Mendes A.R., Soares Silva F.A.G., Mena C., Silva F., Silva C.L.M., Teixeira P. & Poças F., Active Bio-Based Packaging for Fresh-Cut Melon: Antimicrobial Efficacy and Zinc Migration of Nanocellulose/ZnO Nanocomposite Films, *Food Control*, <https://doi.org/10.1016/j.foodcont.2026.112219>.

This is a PDF of an article that has undergone enhancements after acceptance, such as the addition of a cover page and metadata, and formatting for readability. This version will undergo additional copyediting, typesetting and review before it is published in its final form. As such, this version is no longer the Accepted Manuscript, but it is not yet the definitive Version of Record; we are providing this early version to give early visibility of the article. Please note that Elsevier's sharing policy for the Published Journal Article applies to this version, see: <https://www.elsevier.com/about/policies-and-standards/sharing#4-published-journal-article>. Please also note that, during the production process, errors may be discovered which could affect the content, and all legal disclaimers that apply to the journal pertain.

© 2026 Published by Elsevier Ltd.

Active Bio-Based Packaging for Fresh-Cut Melon: Antimicrobial Efficacy and Zinc Migration of Nanocellulose/ZnO Nanocomposite Films

Ana Rita Mendes¹, Francisco A.G. Soares Silva¹, Cristina Mena², Fátima Silva², Cristina L. M. Silva¹, Paula Teixeira¹, Fátima Poças^{1,2,*}

¹Universidade Católica Portuguesa, CBQF - Centro de Biotecnologia e Química Fina – Laboratório Associado, Escola Superior de Biotecnologia, Rua Diogo Botelho 1327, 4169-005 Porto, Portugal; s-anrimamendes@ucp.pt (A.R.M.)

²CINATE, Escola Superior de Biotecnologia, Universidade Católica Portuguesa, Rua Diogo Botelho 1327, 4169-005 Porto, Portugal

*Correspondence: fpocas@ucp.pt

Abstract

Growing environmental concerns, together with the need to extend shelf life and protect food from pathogens and mechanical damage, are driving the development of innovative active packaging materials. In this study, nanocellulose (NC) films incorporating zinc oxide nanoparticles (ZnO NPs) with three different morphologies (spherical, sheet and flower) were produced by solvent casting for food packaging applications. Films were characterised by scanning electron microscopy (SEM), and antimicrobial activity was addressed by agar diffusion assay against *Escherichia coli* and *Staphylococcus aureus*. NC/ZnO films were used as package for fresh-cut melon, which was stored at 4 °C for one week, and subjected to microbiological, pH and zinc migration analysis.

SEM revealed a porous, and nanofibrillar cellulose, suitable for NP retention, while cross sections showed the dispersion of NPs among the films. *In vitro* antimicrobial studies demonstrated the influence of morphology, with the sheet shape producing the highest inhibitory halos. In contact with melon, NC/ZnO films suppressed microbial proliferation relative to controls, keeping microbiological levels within acceptable limits up to day 7. Sheet shape showed the most significant effect. Total Zn migration plateaued at 7–8 mg kg⁻¹ under a realistic area-to-mass scenario, with no significant differences among morphologies. Measurements reflect total Zn after acid digestion and ionic versus particulate species could not be distinguished. NC/ZnO films maintained slightly higher pH than controls.

Overall, these findings highlight the potential of bio-based NC/ZnO films to extend melon shelf life, with antimicrobial efficacy strongly influenced by nanoparticle morphology.

36

37 **Keywords:** zinc oxide nanoparticles; active food packaging; shelf life extension; fresh-cut melon;
38 zinc migration; nanocellulose films; bio-based materials.

39

40 1. Introduction

41 Consumers are increasingly interested in minimally processed foods due to their health
42 benefits. Fresh fruits and vegetables are a priority in many purchasing decisions, as they provide
43 vitamins, minerals, dietary fibre, and antioxidants that support a balanced diet (Török et al.,
44 2023). However, these foods are unstable after harvesting due to physical damage, biochemical
45 changes, moisture loss, microbial proliferation, and oxidative deterioration, compromising
46 quality and shelf life (Venkatesan & Muniyan, 2024). Packaging plays an important role in
47 preserving product quality during storage, handling, and final use. In particular, active packaging
48 has gained significant attention for its ability to extend shelf life, preserve freshness, and enhance
49 safety by limiting the growth of potentially hazardous bacteria (Ahmed et al., 2022; Fadiji et al.,
50 2023; Pascall, 2020). Additionally, by reducing spoilage, active packaging can also help in
51 decreasing food waste and lowering corresponding environmental impacts. Growing global
52 concern about sustainability is driving the replacement of petroleum-based plastics with bio-
53 based, environmentally friendly materials (Basumatary et al., 2022; Dejene et al., 2024).

54 Within this context, nanocellulose (NC) is a natural polymer derived from various plants and
55 agricultural products, increasingly used for paper and paperboard, biomedical products, food
56 packaging, and textiles (Zhang et al., 2023). Nanofibrillated cellulose comprises long, flexible
57 fibrils with at least one dimension in the nanometre range, containing abundant hydroxyl groups
58 that enable surface modifications and strong bonding networks (Hansini et al., 2025; Soares Silva
59 et al., 2020). The resulting porous matrix is an effective carrier for active compounds as it
60 stabilises inorganic fillers and metal ions via hydrogen bonding through electrostatic interactions
61 (Kumar et al., 2025; Roy et al., 2021). For food contact applications, cellulose is also used as
62 reinforcing agent to improve physicochemical and functional properties (Maloufi et al., 2025;
63 Singh et al., 2025).

64 Zinc oxide nanoparticles (ZnO NPs) stand out for their broad-spectrum of antimicrobial
65 activity, UV blocking capability, and high surface-to-volume ratio, and are therefore of interest to
66 be incorporated into bio-based polymers for food contact materials (FCM) (Lebaka et al., 2025;
67 Dejene et al., 2025). Antimicrobial efficacy is strongly dependent on particle size and
68 morphology, which modulate the reactive oxygen species (ROS) generation and Zn²⁺ release.
69 Together, these pathways disrupt bacterial cells, inhibiting their proliferation (Kim et al., 2022;

70 Mendes et al., 2025). Despite these functional advantages, potential Zn migration raises
71 concerns about toxicological risk against human health and regulatory compliance. Presently,
72 ZnO (nano) is considered safe by the European Food Safety Authority (EFSA), as an ultraviolet
73 light absorber for plastic FCM (EFSA, 2016). Although extensive literature has documented the
74 antimicrobial role of ZnO and its migration into food simulants (Bumbudsanpharoke et al., 2019;
75 Peter et al., 2022; Singh et al., 2024), studies addressing migration into real food models are
76 scarce. Most available data relate to meat products, particularly poultry (Sasidharan et al., 2024;
77 Soares Silva et al., 2023; Souza et al., 2020).

78 To address this gap, melon fruit was selected for shelf life studies because it has high water
79 activity, which promotes rapid microbial growth even under refrigeration. In addition, melon is
80 commonly commercialized and highly appreciated by consumers in a ready-to-eat cube format,
81 which increases its exposed surface area and, consequently, accelerates microbial spoilage.
82 Therefore, developing a packaging system that enables the assessment of antimicrobial efficacy
83 and zinc migration is particularly relevant. Most previous studies on active packaging for melon
84 have focused on chitosan- or alginate-based films incorporated with silver nanoparticles (NPs),
85 mainly assessing quality attributes, microbial safety, and sensory evaluation (Danza et al., 2015;
86 Ortiz-Duarte et al., 2019; Sun et al., 2022). Only one study has tested cellulose absorbent pads
87 containing silver NPs (Fernández et al., 2010), and studies using ZnO NPs or investigating
88 nanoparticle migration into melon are absent, underscoring the novelty of the present work. In
89 fact, ZnO NPs offer advantages over silver, as they combine lower toxicity and lower production
90 cost with a more sustainable production process (Karuppan Perumal et al., 2025).

91 Regarding the legislative framework, Regulation (EU) No. 2073/2005 lays down
92 microbiological criteria for foodstuffs, providing a well-established control standard for microbial
93 hazards (European Commission, 2005). In contrast, there is a concern and regulatory gap
94 regarding safety of NPs if their migration occurs. According to Regulation (EU) No. 1935/2004,
95 FCM must not release their constituents into food in quantities that could compromise human
96 health, cause unacceptable changes in the food's composition, or deteriorate its organoleptic
97 characteristics (European Commission, 2004). For plastic materials, Regulation (EU) No. 10/2011
98 sets a specific migration limit (SML) for ionic zinc of 5 mg kg^{-1} of food, while indicating that
99 nanoparticles require a case-by-case risk assessment (European Commission, 2011).
100 Additionally, EFSA reported that ZnO NPs do not migrate in nanoparticulate form when
101 incorporated in an unplasticized polymer, so safety assessment should focus on soluble ionic zinc
102 (Zn^{2+}) (EFSA, 2016). However, these assessments were performed only for plastic materials,
103 where the NPs are strongly embedded in the polymeric matrix. In more porous systems, such as
104 cellulose-based materials (ex, films or absorption pads), different migration profiles can occur,

105 requiring case-by-case risk assessment. In fact, a previous study concluded that both ionic Zn
106 and nanoparticle ZnO migrated from nanocellulose films into food simulants (Mendes et al.,
107 2026). Therefore, additional research using real food models is needed to address this regulatory
108 gap and complement the existing regulatory framework (Poças & Franz, 2018).

109 In this context, the present work aims to develop NC nanocomposites incorporating ZnO NPs
110 with three morphologies (spherical, sheet, and flower) and evaluate their performance in a
111 fresh-cut melon model. The films were first characterised regarding their structure and
112 nanoparticle distribution, and agar diffusion assays were performed to confirm *in vitro*
113 antimicrobial efficacy. The films were then applied to melon slices and stored under refrigeration
114 over one week. Microbiological counts and pH were monitored for shelf life assessment. Total
115 Zn migration over time was quantified by atomic absorption spectrometry (AAS) after acid
116 digestion, providing a realistic exposure scenario in a real-food matrix. By combining microbial
117 shelf life studies with migration analysis, this study provides new data on the safety and
118 functionality of bio-based NC/ZnO nanocomposite packaging. The results are expected to
119 contribute to the current knowledge gap between studies using food simulants and those in real
120 food systems, and to support regulatory assessment of nanomaterials in food contact
121 applications.

122

123 **2. Materials and Methods**

124 **2.1. Preparation of NC/ZnO NPs Nanocomposite Films**

125 The ZnO NPs employed in this work were synthesized via sol-gel method in three different
126 morphologies: spherical (ZnO-SP), flower (ZnO-FL), and sheet shape (ZnO-SH), represented in
127 Figure S1. Their physicochemical and functional properties have already been extensively
128 characterized in earlier studies, and a summary of these data is provided in Table S1 (Mendes et
129 al., 2024, 2025).

130 NC/ZnO composite films were obtained through the solvent casting technique. The
131 nanocellulose Valida S231C 3% (Sappi Biochemtech BV, Maastricht, Netherlands) was used. This
132 material originates from wood pulp and presents fibrils with widths between 20 and 60 nm and
133 lengths distribution mainly below 31 μm , as reported by the supplier's technical datasheet.
134 Initially, 1% (w/v) of NC was dispersed in ultrapure water under magnetic stirring for 30 min at
135 room temperature. Glycerol (Sigma-Aldrich, St. Louis, MO, USA) was then incorporated as a
136 plasticizer at 5% (w/w relative to NC dry weight) under constant agitation. Afterwards, each ZnO
137 NPs type was added at 10% (w/w relative to NC dry weight), and homogenized for a further 30
138 min. Subsequently, 32 mL of each formulation was cast into 10x10 cm trays and dried for 48 h
139 under controlled conditions (23 °C, 50% relative humidity). The resulting films were designed

140 according to the incorporated nanoparticle morphology: NC/ZnO-SP, NC/ZnO-FL, and NC/ZnO-
141 SH. Control films without nanoparticles (neat NC) were prepared under identical conditions.
142 Films were cut into discs with a diameter of 13.5 mm for agar diffusion assay, and into 5x5 cm
143 squares for antimicrobial, migration and pH assays using the model food.

144 All composite films were UV irradiated prior to use in antimicrobial assays to reduce surface
145 microbial load. Films were exposed to a bank of four germicidal UV lamps (TUV G30T8, 16 W,
146 Phillips, Amsterdam, Netherlands) with peak emission at 254 nm and an average intensity of
147 12.36 Wm^{-2} , for 10 min. To validate the efficacy of the decontamination process, UV-treated
148 films were placed in direct contact with plate count agar (PCA) (Biokar Diagnostics, Allone,
149 France) plates using sterile tweezers, ensuring full surface contact with the agar. The plates were
150 incubated at 30 °C for 3 days. No microbial growth was observed during this preliminary test,
151 confirming the effectiveness of the UV treatment in eliminating surface contamination (Figure
152 S2). Therefore, this decontamination step was systematically applied to all films prior to
153 microbiological assays.

154 **2.2. Characterisation of NC/ZnO NPs Nanocomposite Films**

155 Valida S231C 3% and NC/ZnO composite films were characterized using a FEI QUANTA 400
156 FEG ESEM (FEI, Hillsboro, OR, USA) microscope equipment, operating at an accelerating voltage
157 of 15 kV. Prior to scanning electron microscopy (SEM) examination, the NC/ZnO films were
158 treated with liquid nitrogen to obtain a clean cut cross-section. Additionally, films were also
159 freeze-dried to observe the fibrillar structure and identify potential sites for ZnO NPs
160 incorporation using a Phenom XL G2 SEM (Thermo Fisher Scientific—FEI, Eindhoven). Prior to
161 testing, samples were frozen at -80 °C and subsequently lyophilized in a freeze dryer (LABCONCO,
162 FreeZone, MO, USA) at -99 °C and 0.025 mbar until completely dry. The analysis was conducted
163 at an accelerating voltage of 15 kV, and a secondary electron detector (SED) was used for
164 micrographs capture.

165 The thickness of the NC/ZnO films was determined using a digital micrometer (Adamel
166 Lhomargy, France) by randomly measuring five distinct points on each sample.

167 **2.3. *In Vitro* Antimicrobial Activity of NC/ZnO Nanocomposite Films**

168 The antimicrobial activity of the NC/ZnO NPs films was assessed by agar diffusion assay
169 against *Escherichia coli* ATCC 8739 and *Staphylococcus aureus* ATCC 6538P. Test bacteria were
170 aseptically inoculated into Tryptic Soy Agar (TSA) (Biokar Diagnostics, Allone, France) plates and
171 incubated at 37 °C for 24 h. Colonies were then harvested with a sterile loop to prepare a cell
172 suspension in brain–heart infusion (BHI) broth (Biokar Diagnostics, Allone, France), which was
173 incubated overnight at 37 °C to obtain a bacterial population of approximately 10^8 – 10^9 CFU mL⁻¹.

174 Subsequently, sterile swabs were immersed in each inoculum suspension and uniformly spread
175 the suspension onto TSA plates. Film discs were then placed directly onto the inoculated plates.
176 After incubation at 37 °C for 24 h, inhibition zones were measured and expressed in mm. The
177 discs were then removed, and the plates were re-incubated at 37 °C, with halos monitored over
178 a 7-day period.

179 **2.4. Fresh Melon Sample Preparation and Packaging**

180 “Pele de Sapo” melons (*Cucumis melon L.*) were purchased from a local Portuguese
181 supermarket and selected based on ripeness, uniform peel colour, and absence of physical
182 damage (Figure 1a). The melons were washed with potable tap water and dried using absorbent
183 paper. All the materials and surfaces were disinfected with ethanol, and the procedures were
184 carried out under aseptic conditions using a Bunsen burner flame. The cleaned fruit was cut with
185 a sterile knife into thin slices after removing the seeds and surrounding spongy tissue. Slices of
186 approximately 10 g were prepared for microbiological analysis and approximately 2 g for
187 migration assay. An extra set of melon slices was prepared for pH measurements. The samples
188 were stored under refrigeration conditions (4 °C).

189 Previously decontaminated NC/ZnO films (5x5 cm) of different morphologies were used to
190 package the melon samples, ensuring full contact between melon surface and the film at all sides
191 of the small melon cube (Figure 1b). The wrapped slices were then placed inside sterile bags and
192 stored under refrigeration conditions (Figure 1c). Microbial, migration, and pH analyses were
193 conducted at five different time points over the course of one week. Triplicate analyses were
194 performed for each nanocomposite type: NC/ZnO-SP, NC/ZnO-FL, NC/ZnO-SH and NC control.

195 **2.4.1. Microbiological Analyses**

196 Total mesophilic aerobic counts at 30 °C and psychrotrophic counts at 7 °C,
197 *Enterobacteriaceae*, and yeast and mould populations were evaluated at days 0, 3, 5, 6, and 7 of
198 the storage period. Under sterile conditions, the NC film was removed from the melon, and a 10
199 g portion of the slice was homogenized for 30 s with 90 mL of Ringer’s solution (Biokar
200 Diagnostics, Allone, France) using a Stomacher SMASHER® Sample Blender (bioMérieux, Marcy-
201 l'Étoile, France). Serial dilutions were prepared in Ringer's solution as required for microbial
202 enumeration. PCA was used for total mesophilic aerobic counts (incubated at 30 °C for 3 days),
203 and for psychrotrophic counts (incubated at 7 °C for 10 days). *Enterobacteriaceae* were
204 quantified using RAPID' *Enterobacteriaceae* Agar (Bio-Rad Laboratories, Marnes-la-Coquette,
205 France) after incubation at 37 °C for 24 h. Yeasts and moulds were enumerated on Dichloran
206 Rose Bengal Chloramphenicol (DRBC) agar (Biokar Diagnostics, Allone, France) following

207 incubation at 25 °C for 5 days. A melon sample without film was used as a control. All microbial
 208 counts were expressed as log colony-forming units per gram of sample (log CFU g⁻¹).

209 **2.4.2. Zinc Migration Analyses**

210 The migration of Zn from NC/ZnO nanocomposite films into melon was assessed over a
 211 storage period of 8 days. Fresh-cut melon samples were collected after 0, 1, 3, 5, and 8 days for
 212 the Zn determination. The Zn concentration was quantified by flame AAS according to standard
 213 EN 14084, following microwave digestion of the whole melon cube. A realistic scenario was
 214 considered, based on the actual surface area-to-mass ratio (A/M) for half a melon (Figure S3).

215 Microwave digestion of 2 g of melon was performed in digestion vessel with the addition of
 216 5 mL of suprapur nitric acid 65% (Panreac, Barcelona, Spain). The samples were then processed
 217 using a microwave digestion system (Speedwave MWS-3+, Berghof, Germany), according to the
 218 program detailed in Table 1. Upon completion of the microwave treatment, the digested samples
 219 were diluted with ultrapure water to a final volume of 50 mL and subsequently analysed by AAS.

220

Table 1 - Microwave digestion program.

Stage	1	2	3	4	5
T (°C)	130	170	200	100	100
Pressure (bar)	20	20	20	20	20
Time (min)	5	10	15	2	2
Ramp (min)	5	5	1	5	1
Power (watt)	30	40	50	30	20

221

222 Zinc quantification was performed using a flame AAS (Perkin Elmer Analyst 400, Waltham,
 223 MA, USA), equipped with a zinc hollow cathode lamp at a wavelength of 213.9 nm.
 224 Measurements were carried out using an air–acetylene flame under standard operating
 225 conditions recommended by the manufacturer. Zinc working standard solutions with 1 % (v/v)
 226 HNO₃, ranging from 0 to 0.50 mg L⁻¹, were prepared from a 1000 mg L⁻¹ standard stock solution
 227 to obtain a calibration curve. Five replicate measurements were performed for each sample and
 228 working solution. System performance was assessed by determining the limit of detection (LOD:
 229 0.008 mg L⁻¹), the limit of quantification (LOQ: 0.025 mg L⁻¹), and recovery (90 - 110%). When
 230 necessary, samples were further diluted with ultrapure water to ensure that the absorbance
 231 signal was within the specified Zn concentration range.

232

233 **2.4.3 pH Determination**

234 Melon samples were collected on days 0, 1, 3, 5, and 7 for pH determination. The samples
 235 were removed from the cold storage, the NC films carefully removed from the slices and the

236 measurements were taken after 3 min at room temperature. The pH of the melon slices was
237 measured using a solid-state pH meter (Mettler Toledo, SevenDirect SD50, Greifensee,
238 Switzerland).

239

240 **2.5. Data Handling and Statistical Analysis**

241 Statistical analysis was performed using IBM SPSS Statistics (version 28), GraphPad Prism
242 (version 10.6.1), and Microsoft Excel. Results were presented as mean \pm standard deviations
243 using tables and graphic representations.

244 One-way analysis of variance (ANOVA) followed by Fisher's least significant difference (LSD)
245 post hoc tests was used to compare inhibition zone diameters among film groups for each
246 microorganism. For the one week experiments (microbiological analysis, Zn migration and pH
247 evaluation), two-factor ANOVA was applied, with storage time (days) and packaging condition
248 (melon control, NC control, NC/ZnO-SP, NC/ZnO-SH, NC/ZnO-FL) as factors. Tuckey's and LSD post
249 hoc tests were used to identify statistically significant differences between each factor. A two-
250 sided $p < 0.05$ was considered statistically significant.

251

252 **3. Results and Discussion**

253 **3.1. Characterisation of NC/ZnO Films**

254 SEM micrographs of the Valida S231C 3% cellulose are represented in Figure 2. Figures 2a,b
255 reveal a relatively homogeneous structure, with fine and long interconnected fibres forming a
256 dense, entangled network. SEM micrographs of the freeze-dried NC matrix show an open, highly
257 porous network composed of interconnected cellulose fibres (Figure 2c,d). The voids and fibre
258 intersections serve as potential sites for ZnO NPs incorporation, enabling their dispersion within
259 the matrix.

260 After incorporating ZnO NPs into the NC matrix, cross-section SEM micrographs of the NC-
261 based films were obtained to evaluate the distribution of ZnO NPs and their impact on the overall
262 film structure (Figure 3). The neat NC film exhibits a compact and homogeneous structure, with
263 no visible particles (Figure 3a,b). This control serves as a reference to assess the structural
264 modifications induced by ZnO NPs incorporation. Regarding the NC/ZnO-SP composite film
265 (Figure 3c,d), the presence of ZnO NPs is evident, but their distribution appears somewhat
266 uneven, with regions showing higher particle concentration. This may indicate partial
267 aggregation of the ZnO NPs within the cellulose matrix. In contrast, the NC/ZnO-FL film (Figure
268 3e,f) exhibits a more homogeneous dispersion of ZnO NPs, with the particles appearing to be
269 better distributed throughout the matrix. The micrographs suggest that ZnO NPs are not only
270 embedded within the NC fibres but also deposited on the surface. Regarding NC/ZnO-SH (Figure

271 3g,h), NPs appear to be well distributed across both the surface and internal regions of the film,
272 with some small particle clusters observed within the layered NC structure. All the films present
273 a torn, layered appearance as they were not rigid enough to fracture cleanly. Nevertheless, this
274 did not hinder the observation of the internal structure and particle distribution.

275 ZnO NPs embedded in the matrix might be bound to the hydroxyl groups of cellulose fibres
276 through hydrogen bonding (Ghule et al., 2006). Comparing the ZnO-loaded films with the neat
277 NC film, it is evident that ZnO NPs incorporation influences the cellulose matrix: an increase in
278 porosity can be observed within the NC network, potentially leading to greater inter-fibre
279 spacing. Additionally, the formation of ZnO NPs clusters in certain regions may introduce
280 structural irregularities that could influence the mechanical integrity of the films. Abbas et al.,
281 2019 reported that a uniform distribution of nanoparticles is crucial for enhancing mechanical
282 properties, whereas aggregation can lead to decreased flexibility and potential defects in the
283 composite structure.

284 The interaction between ZnO NPs and the cellulose matrix is also crucial for evaluating Zn
285 migration. Uniform dispersion of ZnO NPs with strong bonding to the matrix can lead to lower
286 migration rates. In contrast, higher aggregation can alter the structural integrity of the
287 composite, potentially enabling nanoparticle migration (Babakhani, 2019). Furthermore, in areas
288 where ZnO NPs are more exposed to the film surface, a higher release of ZnO over time may be
289 expected. Studies have reported that the extent of NPs exposure on the film's surface plays a
290 significant role in Zn migration behaviour (Bumbudsanpharoke et al., 2019). Excellent
291 compatibility and miscibility between the NC matrix and the filler materials were also observed
292 in cellulose nanofiber-based composite films reinforced with zinc oxide nanorods and grapefruit
293 seed extract (Roy et al., 2021).

294 The thickness of neat NC was $29.6 \pm 1.1 \mu\text{m}$, which slightly increased upon the incorporation
295 of ZnO NPs. Among the samples, NC/ZnO-SH exhibited the highest thickness value (42.0 ± 4.0
296 μm), compared to the films with spherical ($33.4 \pm 4.2 \mu\text{m}$) and flower-shaped ($32.4 \pm 2.5 \mu\text{m}$)
297 ZnO NPs incorporation. This increase confirms that the incorporation of fillers into the film matrix
298 influences its thickness, as previously reported (Ahmadi et al., 2021). This trend aligns with prior
299 findings, in which the incorporation of ZnO NPs into chitosan-based films resulted in a gradual
300 increase in thickness from $42.0 \mu\text{m}$ to $59.3 \mu\text{m}$, depending on the ZnO NPs concentration (Souza
301 et al., 2021). Another study reported that incorporating Fe_3O_4 NPs into the cellulosic matrix
302 increased the distance between cellulose fibres in the cross-section of the films, thereby
303 increasing film thickness (Furlan et al., 2019).

304

3.2. Antimicrobial Activity of NC/ZnO Nanocomposite Films

The antimicrobial activity of the different NC/ZnO films was evaluated against gram-negative *E. coli* and gram-positive *S. aureus* using an agar diffusion assay. The results are presented in Table 2 and Figure 4. Incorporation of ZnO NPs into NC films enhanced antimicrobial efficacy compared to neat NC, particularly against *S. aureus*, although the magnitude of the effect depended on nanoparticle shape.

Among the tested morphologies, sheet-shaped ZnO NPs produced the strongest inhibitory effect against both bacteria, followed by spherical shape; flower-like particles showed only limited or negligible effect. For *S. aureus*, the NC/ZnO-SP and NC/ZnO-SH films produced inhibition zones of 20.5 ± 1.0 and 21.8 ± 1.2 mm, respectively, compared with 17.1 ± 4.2 mm for the NC control. In contrast, the NC/ZnO-FL film produced a smaller inhibition zone (16.1 ± 1.0 mm) than the control. Statistical analysis revealed overall differences among films (one-way ANOVA, $p < 0.05$). NC/ZnO-SH films showed significantly larger inhibition zones than neat NC (Fisher's LSD test, $p < 0.05$). Conversely, NC/ZnO-FL films produced significantly smaller zones than both NC/ZnO-SP and NC/ZnO-SH (Fisher's LSD test, $p < 0.05$), indicating lower antibacterial efficacy against *S. aureus*. Although neat NC films exhibited initial antimicrobial activity, bacterial regrowth was observed within the inhibition zone upon disc removal after 48 h, indicating that the effect was not maintained. In contrast, inhibition zone corresponding to the films containing ZnO NPs maintained clear and stable aspect for at least 7 days, confirming their long-term antimicrobial performance.

For *E. coli*, NC/ZnO-SH and NC/ZnO-SP films produced the largest inhibition zones (17.5 ± 0.3 and 16.9 ± 1.1 mm, respectively), while NC/ZnO-FL and neat NC film produced smaller zones (11.4 ± 5.6 and 10.5 ± 5.4 mm, respectively). However, differences among films were not statistically significant (one-way ANOVA, $p = 0.126$). After disc removal, no bacterial regrowth was observed in any inhibition zone, including those produced by the NC control, for at least 7 days. This apparent absence may be partially influenced by the hygroscopic and adhesive nature of NC, which can retain moisture and physically entrap bacterial cells, thereby potentially preventing the visualization of colonies (Solhi et al., 2023). Another possible explanation is a baseline antimicrobial activity of the neat NC film, attributed to the presence of the 1,2-Benzisothiazolin-3-one, a cellulose dispersion additive with well-documented antimicrobial properties against bacteria, fungi, and yeast (Liu et al., 2025; Viani et al., 2017). Incorporating ZnO NPs, especially those in the SH and SP morphologies, further enhanced the effect, resulting in larger and more uniform inhibition zones.

These findings are consistent with previous reports on ZnO NPs tested in suspension (Mendes et al., 2024, 2025), in which SP and SH morphologies demonstrated superior

340 antimicrobial activity compared with FL. When incorporated into NC films, however, the ZnO-FL
 341 antibacterial effect was almost completely suppressed, suggesting that the NC matrix plays a
 342 critical role in modulating ZnO antimicrobial activity. Notably, in some cases NC/ZnO-FL films
 343 even displayed smaller inhibition zones than neat NC, indicating that the presence of FL particles
 344 may also attenuate the intrinsic antimicrobial activity of the NC matrix. This effect could arise
 345 from the three-dimensional geometry of FL particles, which may become entrapped within the
 346 fibrillar cellulose network, thereby hindering the diffusion of antimicrobial agents. Such
 347 interference may affect not only the release of Zn²⁺ ions and ROS from the FL particles, but also
 348 the diffusion of compounds inherently present in neat NC (benzisothiazolinone). Indeed, our
 349 previous work demonstrated that ZnO-FL possesses a significantly lower specific surface area
 350 compared with ZnO-SP and ZnO-SH particles (Mendes et al., 2024), further supporting their
 351 reduced antimicrobial performance. In contrast, SP and SH nanoparticles offer great surface area
 352 and more efficient Zn²⁺/ROS release, which explains the larger inhibition zones observed.

353 In this study, *S. aureus* (gram-positive) was more susceptible to ZnO NPs than *E. coli* (gram-
 354 negative). This difference is likely due to the structural differences in their cell walls, as the outer
 355 lipopolysaccharide membrane of gram-negative bacteria acts as an additional barrier that limits
 356 the penetration of antimicrobial agents, such as Zn²⁺ ions and ROS (Babayevska et al., 2022). This
 357 trend contrasts with our previous findings in suspension (Mendes et al., 2025), where freely
 358 dispersed ZnO NPs produced greater activity against *E. coli* than against *S. aureus*. In suspension,
 359 rapid Zn²⁺ release, enhanced particle–cell interactions, and ROS generation likely account for the
 360 stronger effect on *E. coli*, which is often more vulnerable to oxidative stress (Behera et al., 2024).
 361 However, when ZnO NPs are embedded in NC films, nanoparticle mobility and ion release are
 362 restricted, and the diffusion-based nature of the agar assay further limits the availability of
 363 antimicrobial agents. Under these conditions, the outer membrane of *E. coli* may provide
 364 additional protection, while *S. aureus*, lacking this outer layer, is comparatively more affected.
 365 Similar findings have been reported for bacterial cellulose films incorporated with ZnO NPs
 366 (Shahmohammadi Jebel & Almasi, 2016), although that study used commercial particles and did
 367 not examine NP morphology. In contrast, in the present study the NC control exhibited some
 368 baseline antimicrobial activity, which may have influenced the comparative outcomes.

369 **Table 2** - Antimicrobial activity of NC/ZnO films determined by agar diffusion assay. Results are expressed as
 370 inhibitory halos (mm).

371

Microorganism	Neat NC	NC/ZnO-SP	NC/ZnO-SH	NC/ZnO-FL
<i>S. aureus</i> ATCC 6538P	17.1 ± 4.2	20.5 ± 1.0	21.8 ± 1.2	16.0 ± 1.0

<i>E. coli</i> ATCC 8739	10.5 ± 5.4	16.9 ± 1.1	17.5 ± 0.3	11.4 ± 5.6
-----------------------------	------------	------------	------------	------------

Values represent the mean ± SD of three independent experiments, each performed in technical triplicate (three discs per plate; two diameter readings per disc).

372

373 3.3. Shelf Life Evaluation of Fresh Melon Packaged with NC/ZnO Films

374 3.3.1. Microbial Growth Monitoring

375 To evaluate the applicability of NC/ZnO films as a packaging material for extending food shelf
 376 life, microbiological analyses were performed on fresh-cut melon samples stored at 4 °C for 7
 377 days. As expected, both the melon control and the neat NC control showed increasing microbial
 378 counts during storage, with counts consistently higher than those observed for melons packaged
 379 with NC/ZnO films across all microbial groups (Figure 5). Notably, the melon with NC control
 380 exhibited approximately 1 log CFU g⁻¹ higher microbial counts than the melon control alone.
 381 Although neat NC films displayed antimicrobial activity in the agar diffusion assay, likely due to
 382 the presence of 1,2-Benzisothiazolin-3-one, this effect was not evident in the melon storage
 383 tests, where microbial growth was even more pronounced. This apparent divergence can be
 384 attributed to differences between the two experimental systems. In the agar diffusion assay,
 385 antimicrobial compounds can easily diffuse through the agar medium because of its simple
 386 matrix nature, facilitating the formation of inhibition zones. In contrast, in real food systems such
 387 as fresh-cut melon, the diffusion of such compounds from the film to food surface may be
 388 limited. In fact, the composition of the melon is a complex interaction of carbohydrates, fibers,
 389 minerals, etc. Additionally, the NC film may reduce surface water loss and maintain a more humid
 390 environment around the melon surface, which can favour microbial proliferation (Ahmad &
 391 Siddiqui, 2015). Furthermore, interactions with the natural microbiota of melon may reduce the
 392 effectiveness of weak antimicrobial compounds. Together, these factors may mask the intrinsic
 393 antimicrobial effect observed for neat NC.

394 Melon samples packaged with NC/ZnO films exhibited a clear reduction in microbial growth
 395 throughout storage, confirming the antimicrobial efficacy of the ZnO-containing films. However,
 396 the magnitude of this effect strongly depended on nanoparticle morphology. NC/ZnO-SH films
 397 were the most effective, maintaining the lowest microbial counts, followed by spherical particles,
 398 while flower-shaped particles exhibited only limited activity. These results are consistent with
 399 the agar diffusion assay and with previous reports on ZnO NPs tested in suspension (Mendes et
 400 al., 2024, 2025), in which SP and SH morphologies demonstrated superior antimicrobial activity,
 401 whereas FL displayed poor antimicrobial performance.

402 Initial populations of total mesophilic aerobic bacteria at 30 °C and 7 °C were approximately
403 2 and 1 log CFU g⁻¹, respectively, while *Enterobacteriaceae* as well as yeasts and moulds were
404 below the detection limit, indicating the good initial microbiological quality of the fresh-cut
405 melon. For total aerobic counts at 30 °C and 7 °C (Figure 5a,b), both storage time and packaging
406 condition had a statistically significant effect on microbial counts ($p < 0.05$). However, the
407 interaction between the two factors was only significant at 30 °C. Counts steadily increase in the
408 control samples, reaching values close to or above 10⁵ CFU g⁻¹ by day 7, which corresponds to
409 the upper acceptability limit for fresh-cut fruits (INSA, 2019; Oms-Oliu et al., 2010). In contrast,
410 melon samples packaged with NC/ZnO films exhibited lower counts throughout storage. At 30
411 °C, all ZnO films resulted in statistically significant reductions in counts on day 7 compared with
412 the cellulose control ($p < 0.05$). In particular, NC/ZnO-SH films were the most effective, with final
413 counts of approximately 10² CFU g⁻¹, which were significantly lower than those of all other study
414 groups (controls and the other ZnO films, $p < 0.05$). On the other hand, NC/ZnO-FL initially
415 delayed microbial proliferation (at day 3, compared with NC control, $p < 0.05$), but this effect was
416 not sustained, and by day 7, they displayed the highest microbial loads among the three
417 morphologies, confirming their poor antimicrobial performance. At 7 °C (Figure 5b), the control
418 groups (melon and NC film) were significantly higher than the ZnO-containing film groups ($p <$
419 0.05).

420 *Enterobacteriaceae* became detectable in the control samples after day 3 and increased
421 sharply until the end of storage (Figure 5c). In the NC/ZnO films, detectable viable
422 microorganisms appeared later during storage, and the microbial growth increased more slowly,
423 remaining lower than in the controls. The interaction between packaging condition and storage
424 time for *Enterobacteriaceae* counts was significant ($p < 0.05$). Higher counts were observed in
425 melon packaged with NC films, reaching values of 10⁵ CFU g⁻¹ by day 7, which corresponds to the
426 upper acceptability limit for fresh-cut fruits. According to microbiological guidelines, satisfactory
427 levels of *Enterobacteriaceae* should remain below 10⁴ CFU g⁻¹ (INSA, 2019; Oms-Oliu et al.,
428 2010). In contrast, populations remained very low or undetectable in melons packaged with
429 NC/ZnO films, particularly with the SH morphology. On day 7, differences were observed for all
430 three ZnO morphologies compared with both melon and NC controls ($p < 0.05$). Although
431 *Enterobacteriaceae* are primarily used as hygiene indicators (relevant to initial contamination
432 and processing), their marked inhibition during storage is also important because members of
433 this group include potential foodborne pathogens (Schwan et al., 2022).

434 Yeasts and moulds also showed progressive growth in the control samples, reaching
435 approximately 4 log CFU g⁻¹ after 7 days, whereas their proliferation was significantly reduced in
436 the presence of ZnO-containing films (Figure 5d). There were no statistically significant

437 differences in counts across packaging groups, nor any interaction between time and packaging
438 groups. However, the effect of time showed that after one week, yeast and mould counts were
439 significantly higher than at earlier time points ($p < 0.05$). According to microbiological guidelines,
440 counts below 10^4 CFU g^{-1} are considered satisfactory, and all samples complied with this limit
441 throughout the 7-day storage period (INSA, 2019; Oms-Oliu et al., 2010). Yeasts and moulds are
442 generally present at lower levels than total mesophilic aerobic bacteria in fresh-cut melon, as
443 previously reported by Ukuku et al., 2018, which is consistent with the trends observed in the
444 present study.

445 In a previous study, cellulose-based absorbent pads containing silver nanoparticles, instead
446 of ZnO-NPs, were applied to fresh-cut melon (Fernández et al., 2010). In that work, microbial
447 growth in melon pieces was only moderately reduced: approximately $0.8 \log$ CFU g^{-1} for total
448 aerobic counts at 30 and 7 °C. This can be explained by the indirect contact of the silver-loaded
449 pads with the fruit, as they became active mainly after being impregnated with melon exudates,
450 thereby limiting their direct antimicrobial effect on the fruit surface. In contrast, the NC/ZnO
451 films in the present study remained in continuous contact with the melon, leading to greater
452 reductions in microbial counts. Similar antimicrobial trends in fresh-cut melon have been
453 reported when incorporating silver NPs into other biopolymeric matrices, such as chitosan (Ortiz-
454 Duarte et al., 2019) and alginate (Danza et al., 2015). However, the magnitude of microbial
455 inhibition varied depending on the polymer and nanoparticle type.

456 The stronger antimicrobial effect observed in this study, particularly for the ZnO-SH films,
457 can be explained by the multiple antimicrobial mechanisms of ZnO NPs. These include the
458 release of Zn^{2+} ions, the generation of ROS, which induce oxidative damage to cellular
459 components, and the direct contact of nanoparticles with microbial membranes, leading to
460 structural disruption. The superior performance of the SH morphology can be attributed to its
461 higher specific surface area, and the continuous contact of the films with the melon surface likely
462 promoted enhanced Zn^{2+} release and ROS generation, thereby reinforcing their antimicrobial
463 activity (Mendes et al., 2024). In contrast, FL showed lower surface area and poorer complex
464 interactions with the matrix, reducing ion/ROS flux and direct cell contact.

465 In summary, these results clearly demonstrate that the incorporation of ZnO NPs delays
466 microbial proliferation in fresh-cut melon, thereby extending its microbiological shelf life.
467 NC/ZnO-SH films effectively maintained safe microbial levels for at least 7 days under
468 refrigerated storage, whereas control samples reached the upper acceptability limit within 3–4
469 days. These findings highlight the potential of ZnO-containing cellulose films as active packaging
470 materials to improve food safety, prolong shelf life, and reduce food waste in minimally
471 processed fruits.

472

473 3.3.2. Evaluation of Zinc Migration in Packaged Melon

474 Zinc migration from NC/ZnO nanocomposite films into melon was assessed under realistic
475 conditions. The results showed that melons in contact with all NC/ZnO films exhibited a similar
476 migration profile, characterized by a rapid increase during the initial days of storage, followed by
477 a stabilization after day 4 (Figure 6). This trend suggests an initial fast diffusion of loosely bound
478 or surface-available Zn species, followed by the establishment of equilibrium between the film
479 and food matrix. Although the three morphologies exhibited distinct particle sizes and specific
480 surface areas, as represented in Figure S1, these differences did not influence Zn migration in
481 the melon matrix. In fact, ZnO NPs morphology can influence dissolution behaviour, as smaller
482 particles with higher surface areas tend to release more Zn²⁺ ions. However, under the present
483 conditions, the migration process appears to be governed primarily by the properties of the food
484 matrix rather than by NPs morphology. The high water content of melon may promote ZnO
485 dissolution and Zn²⁺ release in a similar pattern for all the samples, regardless of NPs and
486 morphology.

487 The SML for Zn (5 mg kg⁻¹ of food) was reached after approximately 2 days, with
488 concentrations further increasing to 7 - 8 mg kg⁻¹ melon. These levels exceeded the migration
489 limit, underscoring the importance of carefully controlling the interaction between ZnO NPs and
490 the food matrix, as balancing antimicrobial efficacy with regulatory compliance is essential for
491 the safe application of such materials in food packaging. It is important to note that the
492 experimental setup represents a high contact surface area scenario, involving direct exposure of
493 a small melon portion to a relatively large film area, which increases migration compared to
494 typical packaging conditions. Therefore, these results should not be interpreted as an automatic
495 disqualification of ZnO nanocomposites for food packaging applications. These findings
496 represent a worst-case scenario and underscore the need for further optimization of overall
497 packaging, considering that Zn migration behaviour strongly depends on several factors,
498 including NPs loading, NPs/matrix interaction, food composition, storage time, temperature, and
499 the surface area-to-mass ratio between packaging and food.

500 The control melon samples exhibited negligible Zn levels throughout the storage period,
501 confirming that the detected Zn was originated from nanocomposite films. Two-way ANOVA
502 revealed statistically significant interaction between storage time and packaging condition
503 groups ($p < 0.05$) on Zn migration. Interaction post-hoc Tukey's test showed that, from day 1
504 onwards, all melons containing NC/ZnO NPs films exhibited significantly higher Zn levels

505 compared to the control ($p < 0.05$), and no significant differences were observed among the
506 different ZnO film morphologies at any time point.

507 The experimental Zn concentration data (Table S2) were converted to realistic packaging
508 conditions based on the actual surface area-to-mass ratio of a half melon. Average melon
509 dimensions of 25x15 cm and a total weight of 4 kg per fruit (2 kg per half fruit) were considered.
510 The edible portion was assumed to extend 4 cm from the surface. After subtracting the seed
511 cavity, the effective contact area was estimated as 2 dm². Normalized to the mass of 2 kg, this
512 corresponded to an A/M ratio of 1 dm² kg⁻¹ (Figure S3). The detailed calculation is provided in
513 supplementary material. No previous studies on packaged melon have assessed the migration
514 of compounds directly to the fruit itself. One study developing cellulose pad with silver NPs
515 demonstrated silver migration into an external medium (Mueller-Hinton Broth) using graphite-
516 furnace atomic absorption spectrometry, rather than directly into the melon matrix (Fernández
517 et al., 2010).

518 The Zn migration profiles observed in melon differed from those previously reported for the
519 same films tested with food simulants (water and 10% ethanol) (Mendes et al., 2026). Higher Zn
520 migration rates were observed in the real food matrix than in food simulants. In water food
521 simulant, the SML was reached only after 29 days, and Zn levels approached 8 mg kg⁻¹ after 35
522 days. In contrast, melon samples reached similar Zn concentrations after only 8 days of storage.
523 Moreover, when using food simulants, a clear difference in Zn migration was observed among
524 the three ZnO morphologies, whereas in melon, all samples exhibited similar migration
525 behaviour. In fact, melon has a complex composition, including organic acids, sugars, high water
526 content, and enzymatic activity, that may facilitate ZnO dissolution and Zn²⁺ release (Youn &
527 Choi, 2022). Studies with ZnO NPs incorporated in bacterial nanocellulose have also
528 demonstrated that Zn migration was much higher in chicken food than in ethanolic food
529 simulants (Soares Silva et al., 2023). This discrepancy highlights the limitations of simulant-based
530 testing as models of real food interactions, although such approaches remain important for
531 regulatory compliance when overestimation is assured (Lerch et al., 2023). It is important to note
532 that migration levels in real foods are expected to vary depending on food type, storage
533 conditions, packaging characteristics, and intrinsic food properties, such as composition, water
534 content, and pH. Under realistic exposure conditions, Zn migration from NC/ZnO films can
535 approach or surpass regulatory migration limits, especially in high-moisture and acidic food
536 matrices. Future studies should therefore extend to different food matrices and packaging
537 systems to better understand the NPs migration variation under real case scenarios. Considering
538 the relatively high Zn concentrations observed in melon, future strategies could also include the
539 application of surface coatings or barrier layers designed to delay Zn migration.

540 Another aspect to consider is that the present study addressed only total Zn migration,
541 without differentiating between ionic Zn^{2+} and nanoparticulate forms. Based on previous results,
542 also for NC films, obtained with food simulants, ca 18% of the total migrated Zn corresponded
543 to ZnO NPs (Mendes et al., 2026). As a rough estimation, a similar ratio can be considered for
544 melon samples. Considering the total Zn migration values of approximately 8 mg kg^{-1} melon, this
545 corresponds to an estimated $1.3 - 1.5 \text{ mg kg}^{-1}$ potentially attributed to ZnO NPs, while the
546 remaining proportion would represent the ionic Zn^{2+} . However, this estimation should be
547 interpreted with caution, as the complex composition of melon (organic acids, sugars, enzymes)
548 may influence ZnO dissolution and migration dynamics, leading to a different ionic/nanoparticle
549 ratio compared with that of food simulants. Differentiating between these two migrating forms
550 is essential for accurate assessment of potential exposure and toxicity, since physicochemical
551 properties, mechanisms and bioavailability of Zn^{2+} ions differ from those of ZnO NPs (EFSA, 2021;
552 Wu et al., 2019). This distinction remains one of the major analytical challenges in the field, as
553 well as regulation gap regarding nanoparticle migration (Ansari et al., 2026). Understanding the
554 type of migration and the release mechanisms is indeed crucial for future toxicological
555 evaluations of these materials.

556

557 **3.3.3. Monitoring of pH in Packaged Melon**

558 One crucial parameter related with microbiological and Zn migration results was the pH
559 evolution of fresh-cut melon in contact with NC/ZnO films, stored at $4 \text{ }^\circ\text{C}$ for 7 days. Results for
560 melon control and melon with nanocomposite films are shown in Figure 7. The initial pH of 6.5
561 exhibited a sharp decrease on the first day, followed by stabilization until day 7 for all the
562 samples. This initial pH drop may be associated with physiological responses triggered by tissue
563 disruption during cutting, which can induce stress and accelerate metabolic processes in fresh-
564 cut fruits, thereby masking the immediate effect of the packaging (Guo et al., 2023). The
565 subsequent observed fluctuations may be attributed to intrinsic variability of the melon
566 metabolic activity, as well as the experimental measurements. Both melon control and the
567 melon-NC control demonstrated a stronger decrease (to approximately 5.8), whereas melons
568 packaged with NC/ZnO films maintained slightly higher pH values after 7 days. Two-way ANOVA
569 showed that storage time and packaging condition significantly affected melon pH values ($p <$
570 0.05), while their interaction was not significant. Post-hoc Tukey's test revealed that melon
571 packaged with NC control film exhibited significantly lower pH compared to melons packaged
572 with NC/ZnO films ($p < 0.05$). The more acidic pH observed in the control samples can be
573 explained by the higher microbial activity (Figure 5), since proliferation of microorganisms
574 producing organic acids and other metabolites contribute to pH reduction and accelerate fruit

575 spoilage. In contrast, melons packaged with ZnO films maintained slightly higher pH values, likely
576 due to microbial growth inhibition. Furthermore, pH is also a key factor influencing ZnO
577 solubilization, as lower pH may promote dissolution and the subsequent release of Zn²⁺ ions
578 (Hakeem et al., 2020). The gradual pH decrease observed over one week may therefore
579 contribute for the increased Zn migration in melons packaged with NC/ZnO films (Figure 6).

580 A similar behaviour of an initial pH decline has been reported for fresh-cut melon fruit
581 packaged with chitosan/graphene oxide films (Paiva et al., 2020). However, that study extended
582 storage to 21 days, revealing a subsequent pH increase after the initial decline, which was not
583 seen in the current work. This implies that multiphase dynamics may influence pH change based
584 on storage duration and microbial activity. In food science, pH is a crucial quality parameter as it
585 influences various aspects such texture, flavour, and microbial stability, while also serving as an
586 indicator of food safety (Venkatesan & Muniyan, 2024). Nevertheless, the intrinsic characteristics
587 of the food matrix, such as water activity and sugar content, can strongly influence the pH
588 evolution. Additionally, extrinsic factors such as initial microbial load and storage conditions can
589 also significantly affect these dynamics. As a result, the present outcomes cannot be directly
590 generalized to other food matrices and should instead be evaluated on a case-by-case basis,
591 considering their specific physicochemical and microbiological properties.

592

593 **4. Conclusion**

594 This work allowed for the development and evaluation of NC films containing three different
595 ZnO NPs morphologies, assessing their capacity to extend melon shelf life, by reducing microbial
596 proliferation, in parallel with zinc migration assessment.

597 SEM micrographs confirmed the nanofibrillar and porous NC network of the films, suggesting
598 an appropriate structure for ZnO NPs linking, and cross-sectional SEM showed the distribution
599 of the ZnO NPs within the matrix. *In vitro* antimicrobial activity of NC/ZnO films was assessed
600 against *S. aureus* and *E. coli*, where results revealed a clear morphology effect: NC/ZnO-SH
601 produced higher inhibitory halos, followed by NC/ZnO-SP, whereas FL films showed lower
602 inhibition. The greater susceptibility of *S. aureus* compared with *E. coli* is consistent with the
603 additional outer membrane of gram-negative *E. coli*, that limits the Zn²⁺/ROS release from NPs.

604 When applied to a fresh-cut melon and stored at 4 °C for one week, NC/ZnO films slowed
605 microbial proliferation compared with neat NC and control melon samples. The effect of NPs
606 morphology was evident: ZnO-SH produced the slowest increase in microbial loads, followed by
607 ZnO-SP, whereas ZnO-FL showed the weakest inhibition among the three shapes. Under a
608 realistic area-to-mass scenario, total Zn reached the SML at day 2 and stabilized by 7–8 mg kg⁻¹,

609 with no differences among morphologies. Melons packaged with NC/ZnO-NPs films presented
610 slightly higher pH compared with NC and melon control, consistent with antimicrobial and Zn
611 migration results.

612 Current EU Regulations and EFSA guidelines were developed for plastics FCM and do not yet
613 fully cover bio-based composites. Moreover, nanoparticle migration in FCM remains
614 insufficiently addressed and is handled on a case-by-case basis for risk assessment. In this study,
615 total Zn was quantified after acid digestion of the whole melon cube, so ionic and particulate
616 forms could not be differentiated. Future work should include particle/ion discrimination using
617 other analytical techniques for quantification, such as single particle inductively coupled plasma
618 mass spectrometry (spICP-MS) or Asymmetric-Flow Field-Flow Fractionation (AF4). Furthermore,
619 it would be valuable to analyse the concentration profile within the melon pulp by determining
620 the Zn levels in direct contact with the film and in regions progressively farther from the contact
621 surface, in order to evaluate the extent of Zn diffusion through the pulp. Additionally, the
622 quantification of the amount of Zn remaining in the film itself after the migration step would
623 have been of interest as a mass balance verification. Moreover, experiments were limited to one
624 food matrix and storage condition. Evaluation of different fruits and storage conditions,
625 combined with toxicological and sensory studies, would be relevant for better assessing
626 consumer safety and acceptance.

627 Overall, NC/ZnO films, particularly those with sheet- and spherical-shaped ZnO NPs,
628 effectively reduced microbial proliferation and maintained microbiological acceptability for at
629 least 7 days, extending food shelf life. Achieving an appropriate balance between antimicrobial
630 performance and zinc migration is required, given the potential toxicological implications. Overall,
631 the effectiveness of bio-based NC/ZnO film is determined by nanomaterial choice, particle
632 morphology, and the properties of the packaging system.

633

634 **Supplementary Materials**

635 The following supporting information can be downloaded at "link". **Figure S1** – SEM (top row)
636 and TEM (bottom row) micrographs of ZnO NPs with different morphologies (Mendes et al.,
637 2024, 2025). **Table S1** - Summary of the main physicochemical and functional properties of ZnO
638 NPs with different morphologies (Mendes et al., 2024, 2025). **Figure S2** - NC/ZnO film placed on
639 a PCA agar plate after UV treatment to confirm the effectiveness of UV sterilization prior to
640 antimicrobial assays. No microbial growth was observed.; **Figure S3** – Schematic and calculation
641 of the area-to-mass (A/M) ratio used for realistic normalization. Assumptions: external
642 dimensions 25x15 cm; edible portion 4 cm; whole fruit mass 4 kg (2 kg per half). After subtracting

643 the seed cavity, effective contact area = 2 dm². Normalized to 2 kg, A/M = 1 dm² kg⁻¹.; **Table S2** -
644 Zn migration (mg kg⁻¹ melon) from NC/ZnO films into fresh-cut melon during storage at 4 °C.
645 Results are expressed as mean ± standard deviation (n = 3). The melon control corresponds to
646 samples stored without contact with the nanocomposite films.

647

648 **CRedit Authorship Contribution Statement**

649 **Ana Rita Mendes:** Investigation, Methodology, Formal analysis, Writing—original draft.

650 **Francisco A.G. Soares Silva:** Investigation, Methodology, Writing—review and editing. **Cristina**

651 **Mena:** Methodology, Writing—review and editing. **Fátima Silva:** Methodology, Writing—review

652 and editing. **Cristina L. M. Silva:** Writing—review and editing. **Paula Teixeira:** Conceptualization,

653 Writing—review and editing. **Fátima Poças:** Supervision, Conceptualization, Resources,

654 Writing—review and editing.

655

656 **Funding**

657 This work was supported by National Funds from FCT - Fundação para a Ciência e a Tecnologia

658 under the scope of project CBQF UID/50016/2025 and the grant UI/BD/151387/2021 (Ana Rita

659 Mendes).

660

661 **Data Availability**

662 Data will be made available on request.

663

664 **Declaration of Competing Interest**

665 The authors declare no conflicts of interest.

666

667 **5. References**

668 Abbas, M., Buntinx, M., Deferme, W., & Peeters, R. (2019). (Bio)polymer/ZnO nanocomposites
669 for packaging applications: A review of gas barrier and mechanical properties. *Nanomaterials*,
670 9, 1494. <https://doi.org/10.3390/nano9101494>

671 Ahmad, M. S., & Siddiqui, M. W. (2015). Factors affecting postharvest quality of fresh fruits. In
672 M. W. Siddiqui (Ed.), *Postharvest quality assurance of fruits* (pp. 7–32). Springer International
673 Publishing. https://doi.org/10.1007/978-3-319-21197-8_2

674 Ahmadi, A., Ahmadi, P., Sani, M. A., Ehsani, A., & Ghanbarzadeh, B. (2021). Functional
675 biocompatible nanocomposite films consisting of selenium and zinc oxide nanoparticles
676 embedded in gelatin/cellulose nanofiber matrices. *International Journal of Biological*
677 *Macromolecules*, 175, 87–97. <https://doi.org/10.1016/j.ijbiomac.2021.01.135>

- 678 Ahmed, Md. W., Haque, Md. A., Mohibullah, Md., Khan, Md. S. I., Islam, M. A., Mondal, Md. H.
679 T., & Ahmmed, R. (2022). A review on active packaging for quality and safety of foods: Current
680 trends, applications, prospects and challenges. *Food Packaging and Shelf Life*, 33, 100913.
681 <https://doi.org/10.1016/j.fpsl.2022.100913>
- 682 Ansari, M. D. I., Principato, L., De Nardo, L., & Punta, C. (2026). Nanomaterials in food packaging:
683 An overview of regulatory frameworks and migration assessment. *Food Control*, 181, 111707.
684 <https://doi.org/10.1016/j.foodcont.2025.111707>
- 685 Babakhani, P. (2019). The impact of nanoparticle aggregation on their size exclusion during
686 transport in porous media: One- and three-dimensional modelling investigations. *Scientific*
687 *Reports*, 9, 14071. <https://doi.org/10.1038/s41598-019-50493-6>
- 688 Babayevska, N., Przysiecka, Ł., Iatsunskyi, I., Nowaczyk, G., Jarek, M., Janiszewska, E., & Jurga, S.
689 (2022). ZnO size and shape effect on antibacterial activity and cytotoxicity profile. *Scientific*
690 *Reports*, 12, 8148. <https://doi.org/10.1038/s41598-022-12134-3>
- 691 Basumatary, I. B., Mukherjee, A., Katiyar, V., & Kumar, S. (2022). Biopolymer-based
692 nanocomposite films and coatings: Recent advances in shelf-life improvement of fruits and
693 vegetables. *Critical Reviews in Food Science and Nutrition*, 62, 1912–1935.
694 <https://doi.org/10.1080/10408398.2020.1848789>
- 695 Behera, S. K., Khan, G. A., Singh, S. S., Jena, B., Sashank, K., Patnaik, S., Kumar, R., Jeon, B.-H.,
696 Chakraborty, S., Tripathy, S. K., & Mishra, A. (2024). Antibacterial efficacy of ZnO/bentonite
697 (clay) nanocomposites against multidrug-resistant *Escherichia coli*. *ACS Omega*, 9, 2783–2794.
698 <https://doi.org/10.1021/acsomega.3c07950>
- 699 Bumbudsanpharoke, N., Choi, J., Park, H. J., & Ko, S. (2019). Zinc migration and its effect on the
700 functionality of a low density polyethylene–ZnO nanocomposite film. *Food Packaging and Shelf*
701 *Life*, 20, 100301. <https://doi.org/10.1016/j.fpsl.2019.100301>
- 702 Danza, A., Conte, A., Mastromatteo, M., & Del Nobile, M. A. (2015). A new example of
703 nanotechnology applied to minimally processed fruit: The case of fresh-cut melon. *Journal of*
704 *Food Processing & Technology*, 6, 1000439. <https://doi.org/10.4172/2157-7110.1000439>
- 705 Dejene, Bekinew Kitaw; Abteu, Mulat Alubel. (2025). Chitosan/zinc oxide (ZnO) nanocomposites:
706 A critical review of emerging multifunctional applications in food preservation and biomedical
707 systems. *International Journal of Biological Macromolecules*, 320, 144773.
708 <https://doi.org/10.1016/j.ijbiomac.2025.144773>
- 709 Dejene, Bekinew Kitaw; Birilie, Alehegn Atalay; Yizengaw, Megabi Adane; Getahun, Samuel;
710 Tadesse, Tesfaye; Tsegaye, Teshome; Tadesse, Belayneh. (2024). Thermoplastic starch-ZnO
711 nanocomposites: A comprehensive review of their applications in functional food packaging.
712 *International Journal of Biological Macromolecules*, 282, 137099.
713 <https://doi.org/10.1016/j.ijbiomac.2024.137099>
- 714 EFSA CEF Panel (EFSA Panel on Food Contact Materials, Enzymes, Flavourings and Processing
715 Aids. (2016). Scientific opinion on the safety assessment of the substance zinc oxide,
716 nanoparticles, for use in food contact materials. *EFSA Journal*, 14, 4408.
717 <https://doi.org/10.2903/j.efsa.2016.4408>
- 718 EFSA Scientific Committee, More, S., Bampidis, V., Benford, D., Bragard, C., Halldorsson, T.,
719 Hernandez-Jerez, A., Hougaard Bennekou, S., Koutsoumanis, K., Lambré, C., Machera, K.,

- 720 Naegeli, H., Nielsen, S., Schlatter, J., Schrenk, D., Silano, V., Turck, D., Younes, M., Castenmiller,
721 J., Chaudhry, Q., Cubadda, F., Franz, R., Gott, D., Mast, J., Mortensen, A., Oomen, A. G., Weigel,
722 S., Barthelemy, E., Rincon, A., Tarazona, J., & Schoonjans, R. (2021). Guidance on risk assessment
723 of nanomaterials to be applied in the food and feed chain: Human and animal health. *EFSA*
724 *Journal*, 19, 6768. <https://doi.org/10.2903/j.efsa.2021.6768>
- 725 European Commission. (2004). Regulation (EC) No 1935/2004 on food contact materials. *Official*
726 *Journal of the European Union*, L338, 4–17. [https://eur-lex.europa.eu/legal-](https://eur-lex.europa.eu/legal-content/EN/TXT/?uri=CELEX:32004R1935)
727 [content/EN/TXT/?uri=CELEX:32004R1935](https://eur-lex.europa.eu/legal-content/EN/TXT/?uri=CELEX:32004R1935)
- 728 European Commission. (2005). *Regulation (EC) No 2073/2005: Microbiological criteria for*
729 *foodstuffs. Official Journal of the European Union*, L338, 1–26. [https://eur-lex.europa.eu/legal-](https://eur-lex.europa.eu/legal-content/EN/TXT/?uri=CELEX:32005R2073)
730 [content/EN/TXT/?uri=CELEX:32005R2073](https://eur-lex.europa.eu/legal-content/EN/TXT/?uri=CELEX:32005R2073)
- 731 European Commission. (2011). *Regulation (EU) No 10/2011 on plastic food contact materials.*
732 *Official Journal of the European Union*, L12, 1–89. [https://eur-lex.europa.eu/legal-](https://eur-lex.europa.eu/legal-content/EN/TXT/?uri=CELEX:32011R0010)
733 [content/EN/TXT/?uri=CELEX:32011R0010](https://eur-lex.europa.eu/legal-content/EN/TXT/?uri=CELEX:32011R0010)
- 734 Fadiji, T., Rashvand, M., Daramola, M. O., & Iwarere, S. A. (2023). A review on antimicrobial
735 packaging for extending the shelf life of food. *Processes*, 11, 590.
736 <https://doi.org/10.3390/pr11020590>
- 737 Fernández, A., Picouet, P., & Lloret, E. (2010). Cellulose-silver nanoparticle hybrid materials to
738 control spoilage-related microflora in absorbent pads located in trays of fresh-cut melon.
739 *International Journal of Food Microbiology*, 142, 222–228.
740 <https://doi.org/10.1016/j.ijfoodmicro.2010.07.001>
- 741 Furlan, D. M., Morgado, D. L., Oliveira, A. J. A. de, Faceto, Â. D., Moraes, D. A. de, Varanda, L. C.,
742 & Frollini, E. (2019). Sisal cellulose and magnetite nanoparticles: Formation and properties of
743 magnetic hybrid films. *Journal of Materials Research and Technology*, 8, 2170–2179.
744 <https://doi.org/10.1016/j.jmrt.2019.02.005>
- 745 Ghule, K., Ghule, A. V., Chen, B.-J., & Ling, Y.-C. (2006). Preparation and characterization of ZnO
746 nanoparticles coated paper and its antibacterial activity study. *Green Chemistry*, 8, 1034–1041.
747 <https://doi.org/10.1039/b605623g>
- 748 Guo, Y., Yu, Z., Li, R., Wang, L., Xie, C., & Wu, Z. (2023). Cut-wounding promotes phenolic
749 accumulation in *Cucumis melo* L. fruit (cv. Yugu) by regulating sucrose metabolism. *Horticulturae*,
750 9, 258. <https://doi.org/10.3390/horticulturae9020258>
- 751 Hakeem, M. J., Feng, J., Nilghaz, A., Ma, L., Seah, H. C., Konkel, M. E., & Lu, X. (2020). Active
752 packaging of immobilized zinc oxide nanoparticles controls *Campylobacter jejuni* in raw chicken
753 meat. *Applied and Environmental Microbiology*, 86, e01195-20.
754 <https://doi.org/10.1128/AEM.01195-20>
- 755 Hansini, A. M. P., Galpaya, G. D. C. P., Gunasena, M. D. K. M., Abeyesundara, P. M., Kirthika, V.,
756 Bhagya, L., Gunawardana, H. D. C. N., & Koswattage, K. R. (2025). From nature to innovation:
757 Advances in nanocellulose extraction and its multifunctional applications. *Molecules*, 30, 2670.
758 <https://doi.org/10.3390/molecules30132670>
- 759 INSA (Instituto Nacional de Saúde Doutor Ricardo Jorge). (2019). *Interpretação de resultados de*
760 *ensaios microbiológicos em alimentos prontos para consumo e em superfícies do ambiente de*

- 761 *preparação e distribuição alimentar: valores-guia*. Instituto Nacional de Saúde Doutor Ricardo
762 Jorge.
- 763 Karuppan Perumal, M. K., Rajasekaran, M. B. S., Rajan Renuka, R., Samrot, A. V., & Nagarajan,
764 M. (2025). Zinc oxide nanoparticles and their nanocomposites as an imperative coating for smart
765 food packaging. *Applied Food Research*, 5, 100849. <https://doi.org/10.1016/j.afres.2025.100849>
- 766 Kim, I., Viswanathan, K., Kasi, G., Thanakkasaranee, S., Sadeghi, K., & Seo, J. (2022). ZnO
767 nanostructures in active antibacterial food packaging: Preparation methods, antimicrobial
768 mechanisms, safety issues, future prospects, and challenges. *Food Reviews International*, 38,
769 537–565. <https://doi.org/10.1080/87559129.2020.1737709>
- 770 Kumar, L., Agwuncha, S. C., Tyagi, P., & Pal, L. (2025). Enhanced chitosan–microfibrillated
771 cellulose hydrogen bonding for edible packaging and food shelf-life extension. *Food Packaging
772 and Shelf Life*, 52, 101613. <https://doi.org/10.1016/j.fpsl.2025.101613>
- 773 Lebaka, V. R., Ravi, P., Reddy, M. C., Thummala, C., & Mandal, T. K. (2025). Zinc oxide
774 nanoparticles in modern science and technology: Multifunctional roles in healthcare,
775 environmental remediation, and industry. *Nanomaterials*, 15, 754.
776 <https://doi.org/10.3390/nano15100754>
- 777 Lerch, M., Fengler, R., Mbog, G.-R., Nguyen, K. H., & Granby, K. (2023). Food simulants and real
778 food – What do we know about the migration of PFAS from paper based food contact materials?.
779 *Food Packaging and Shelf Life*, 35, 100992. <https://doi.org/10.1016/j.fpsl.2022.100992>
- 780 Liu, L., Yuan, M., Huang, J., Geng, L., Wu, N., Yue, Y., Wang, J., & Zhang, Q. (2025). Preparation
781 and antibacterial properties of benzisothiazolinone quaternized chitosan derivatives for
782 sustainable fuel preservation. *Carbohydrate Polymers*, 356, 123379.
783 <https://doi.org/10.1016/j.carbpol.2025.123379>
- 784 Maloufi, M., Djelad, A., Mokhtar, A., Reguig, K., Hasnaoui, M. A., Kebir-Medjhoua, Z. A.,
785 Ghamnia, M., & Sassi, M. (2025). Fabrication and characterization of cellulose-based packaging
786 films with polyethylene glycol and silver nanoparticles for enhanced antimicrobial efficacy.
787 *International Journal of Biological Macromolecules*, 308, 142381.
788 <https://doi.org/10.1016/j.ijbiomac.2025.142381>
- 789 Mendes, A. R., Geiss, O., Bianchi, I., Ponti, J., Matos, A., Silva, C. L. M., & Poças, F. (2026).
790 Migration of ionic and nanoparticulate zinc from nanocellulose/ZnO nanoparticles films:
791 Morphology-dependent behaviour and modelling. *Manuscript submitted for publication*.
- 792 Mendes, A. R., Granadeiro, C. M., Leite, A., Geiss, O., Bianchi, I., Ponti, J., Mehn, D., Pereira, E.,
793 Teixeira, P., & Poças, F. (2025). Functional properties and safety considerations of zinc oxide
794 nanoparticles under varying conditions. *Nanomaterials*, 15, 892.
795 <https://doi.org/10.3390/nano15120892>
- 796 Mendes, A. R., Granadeiro, C. M., Leite, A., Pereira, E., Teixeira, P., & Poças, F. (2024). Optimizing
797 antimicrobial efficacy: Investigating the impact of zinc oxide nanoparticle shape and size.
798 *Nanomaterials*, 14, 638. <https://doi.org/10.3390/nano14070638>
- 799 Oms-Oliu, G., Rojas-Graü, M. A., González, L. A., Varela, P., Soliva-Fortuny, R., Hernando, M. I.
800 H., Munuera, I. P., Fiszman, S., & Martín-Belloso, O. (2010). Recent approaches using chemical
801 treatments to preserve quality of fresh-cut fruit: A review. *Postharvest Biology and Technology*,
802 57, 139–148. <https://doi.org/10.1016/j.postharvbio.2010.04.001>

- 803 Ortiz-Duarte, G., Pérez-Cabrera, L. E., Artés-Hernández, F., & Martínez-Hernández, G. B. (2019).
804 Ag-chitosan nanocomposites in edible coatings affect the quality of fresh-cut melon. *Postharvest*
805 *Biology and Technology*, 147, 174–184. <https://doi.org/10.1016/j.postharvbio.2018.09.021>
- 806 Paiva, C. A., Vilvert, J. C., Menezes, F. L. G., Leite, R. H. de L., Santos, F. K. G., Medeiros, J. F., &
807 Aroucha, E. M. M. (2020). Extended shelf life of melons using chitosan and graphene oxide-based
808 biodegradable bags. *Journal of Food Processing and Preservation*, 44, 14871.
809 <https://doi.org/10.1111/jfpp.14871>
- 810 Pascall, M. A. (2020). The role and importance of packaging and labeling in assuring food safety,
811 quality & compliance with regulations I: Packaging basics. In *Food safety and quality systems in*
812 *developing countries* (pp. 261–283). Elsevier. [https://doi.org/10.1016/B978-0-12-814272-](https://doi.org/10.1016/B978-0-12-814272-1.00006-1)
813 [1.00006-1](https://doi.org/10.1016/B978-0-12-814272-1.00006-1)
- 814 Peter, A., Cozmuta, L. M., Nicula, C., Cozmuta, A. M., Apjok, R., Talasman, C. M., Drazic, G., Peñas,
815 A., Calahorra, A. J., Kamgang Nzekoue, F., Huang, X., Sagratini, G., & Silvi, S. (2022). Barrier
816 properties, migration into the food simulants and antimicrobial activity of paper-based materials
817 with functionalized surface. *Polymers and Polymer Composites*, 30.
818 <https://doi.org/10.1177/09673911221106347>
- 819 Poças, F., & Franz, R. (2018). Overview on European regulatory issues, legislation, and EFSA
820 evaluations of nanomaterials. In *Nanomaterials for food packaging* (pp. 277–300). Elsevier.
821 <https://doi.org/10.1016/B978-0-323-51271-8.00010-3>
- 822 Roy, S., Kim, H. C., Panicker, P. S., Rhim, J.-W., & Kim, J. (2021). Cellulose nanofiber-based
823 nanocomposite films reinforced with zinc oxide nanorods and grapefruit seed extract.
824 *Nanomaterials*, 11, 877. <https://doi.org/10.3390/nano11040877>
- 825 Sasidharan, S., Tey, L.-H., Djearmane, S., Ab Rashid, N. K. M., PA, R., Rajendran, V., Syed, A.,
826 Wong, L. S., Santhanakrishnan, V. K., Asirvadam, V. S., & Antony Dhanapal, A. C. T. (2024).
827 Innovative use of chitosan/ZnO NPs bio-nanocomposites for sustainable antimicrobial food
828 packaging of poultry meat. *Food Packaging and Shelf Life*, 43, 101298.
829 <https://doi.org/10.1016/j.fpsl.2024.101298>
- 830 Schwan, C. L., Molitor, A., Hok, L., Ebner, P., Vipham, J. L., & Trinetta, V. (2022). Quantitative and
831 qualitative assessments of *Enterobacteriaceae*, coliforms, and generic *Escherichia coli* on fresh
832 vegetables sold in Cambodian fresh produce distribution centers. *Food Protection Trends*, 42,
833 107–112. <https://doi.org/10.4315/FPT-21-023>
- 834 Shahmohammadi Jebel, F., & Almasi, H. (2016). Morphological, physical, antimicrobial and
835 release properties of ZnO nanoparticles-loaded bacterial cellulose films. *Carbohydrate Polymers*,
836 149, 8–19. <https://doi.org/10.1016/j.carbpol.2016.04.089>
- 837 Singh, S., Şahin, G., Silva, F. A. G. S., Šinkovec, A., Grkman, J. J., Karlovits, I., & Poças, F. (2025).
838 Development of bio-based coatings incorporating microfibrillated cellulose, lignin and ionomer
839 dispersions for food contact applications. *Packaging Technology and Science*, 38, 613–626.
840 <https://doi.org/10.1002/pts.2906>
- 841 Soares Silva, F. A. G., Bento de Carvalho, T., Dourado, F., Gama, M., Teixeira, P., & Poças, F.
842 (2023). Performance of bacterial nanocellulose packaging film functionalised in situ with zinc
843 oxide: Migration onto chicken skin and antimicrobial activity. *Food Packaging and Shelf Life*, 39,
844 101140. <https://doi.org/10.1016/j.fpsl.2023.101140>

- 845 Soares Silva, F. A. G., Dourado, F., Gama, M., & Poças, F. (2020). Nanocellulose bio-based
846 composites for food packaging. *Nanomaterials*, 10, 2041.
847 <https://doi.org/10.3390/nano10102041>
- 848 Solhi, L., Guccini, V., Heise, K., Solala, I., Niinivaara, E., Xu, W., Mihhels, K., Kröger, M., Meng, Z.,
849 Wohler, J., Tao, H., Cranston, E. D., & Kontturi, E. (2023). Understanding nanocellulose–water
850 interactions: Turning a detriment into an asset. *Chemical Reviews*, 123, 1925–2015.
851 <https://doi.org/10.1021/acs.chemrev.2c00611>
- 852 Souza, V. G. L., Alves, M. M., Santos, C. F., Ribeiro, I. A. C., Rodrigues, C., Coelho, I., & Fernando,
853 A. L. (2021). Biodegradable chitosan films with ZnO nanoparticles synthesized using food
854 industry by-products—Production and characterization. *Coatings*, 11, 646.
855 <https://doi.org/10.3390/coatings11060646>
- 856 Souza, V. G. L., Rodrigues, C., Valente, S., Pimenta, C., Pires, J. R. A., Alves, M. M., Santos, C. F.,
857 Coelho, I. M., & Fernando, A. L. (2020). Eco-friendly ZnO/chitosan bionanocomposites films
858 for packaging of fresh poultry meat. *Coatings*, 10, 110.
859 <https://doi.org/10.3390/coatings10020110>
- 860 Singh, S., Pereira, J., Guerreiro, P., Selbourne, C., Paula, C., Cunha, A., Sousa, C., & Poças, F.
861 (2024). Safety profile of ZnO active packaging PBAT-based biomaterial for food packaging: First
862 tier evaluation. *Food Control*, 161, 110389. <https://doi.org/10.1016/j.foodcont.2024.110389>
- 863 Sun, J., Li, Y., Cao, X., Yao, F., Shi, L., & Liu, Y. (2022). A film of chitosan blended with ginseng
864 residue polysaccharides as an antioxidant packaging for prolonging the shelf life of fresh-cut
865 melon. *Coatings*, 12, 468. <https://doi.org/10.3390/coatings12040468>
- 866 Török, Á., Yeh, C.-H., Menozzi, D., Balogh, P., & Czine, P. (2023). European consumers'
867 preferences for fresh fruit and vegetables – A cross-country analysis. *Journal of Agriculture and*
868 *Food Research*, 14, 100883. <https://doi.org/10.1016/j.jafr.2023.100883>
- 869 Ukuku, D. O., Mukhopadhyay, S., & Olanya, M. (2018). Reducing transfer of *Salmonella* and
870 aerobic mesophilic bacteria on melon rind surfaces to fresh juice by washing with chlorine: Effect
871 of waiting period before refrigeration of prepared juice. *Frontiers in Sustainable Food Systems*,
872 2, 78. <https://doi.org/10.3389/fsufs.2018.00078>
- 873 Venkatesan, U., & Muniyan, R. (2024). Review on the extension of shelf life for fruits and
874 vegetables using natural preservatives. *Food Science and Biotechnology*, 33, 2477–2496.
875 <https://doi.org/10.1007/s10068-024-01602-3>
- 876 Viani, F., Rossi, B., Panzeri, W., Merlini, L., Martorana, A. M., Polissi, A., & Galante, Y. M. (2017).
877 Synthesis and antibacterial activity of a library of 1,2-benzisothiazol-3(2H)-one (BIT) derivatives
878 amenable to crosslinking to polysaccharides. *Tetrahedron*, 73, 1745–1761.
879 <https://doi.org/10.1016/j.tet.2017.02.025>
- 880 Wu, F., Harper, B. J., & Harper, S. L. (2019). Comparative dissolution, uptake, and toxicity of zinc
881 oxide particles in individual aquatic species and mixed populations. *Environmental Toxicology*
882 *and Chemistry*, 38, 591–602. <https://doi.org/10.1002/etc.4349>
- 883 Youn, S.-M., & Choi, S.-J. (2022). Food additive zinc oxide nanoparticles: Dissolution, interaction,
884 fate, cytotoxicity, and oral toxicity. *International Journal of Molecular Sciences*, 23, 6074.
885 <https://doi.org/10.3390/ijms23116074>

886 Zhang, F., Shen, R., Li, N., Yang, X., & Lin, D. (2023). Nanocellulose: An amazing nanomaterial
887 with diverse applications in food science. *Carbohydrate Polymers*, 304, 120497.
888 <https://doi.org/10.1016/j.carbpol.2022.120497>

Journal Pre-proof

Figures



Figure 1 – Experimental procedure with melon samples: a) whole melon fruits purchased from a local Portuguese supermarket; b) melon slice (~3x3 cm) wrapped with the NC/ZnO film (5x5 cm); c) wrapped samples corresponding to one of the five experimental time points, stored in sterile bags for subsequent analysis.

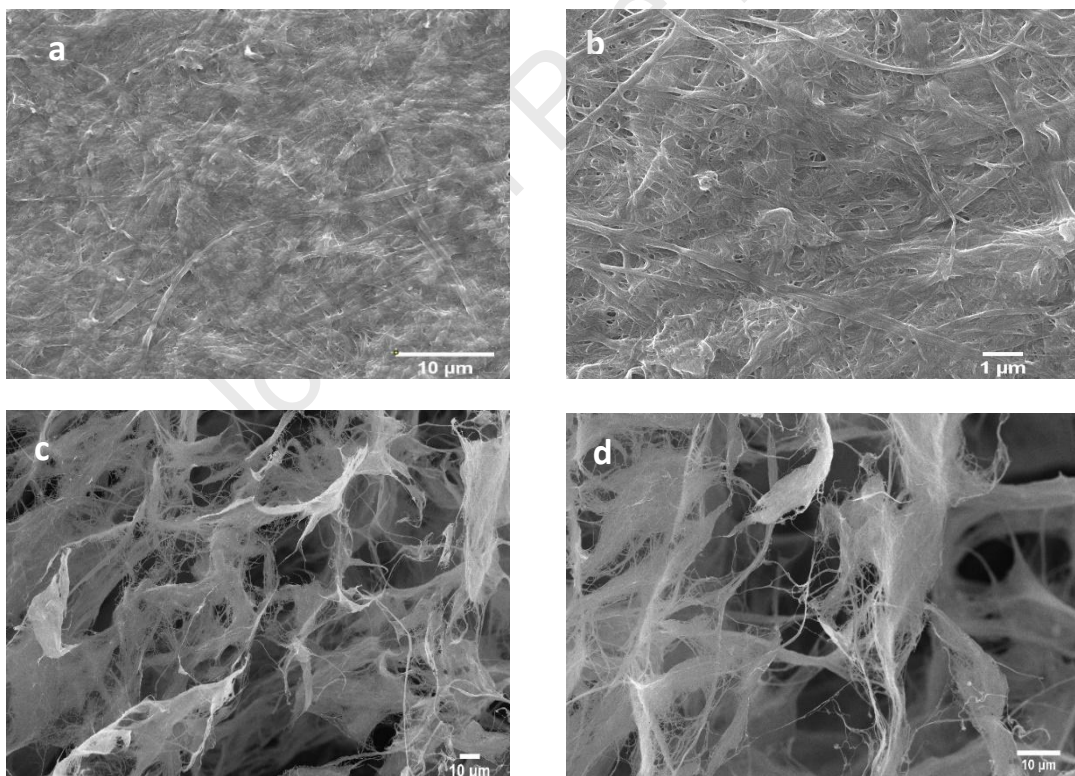


Figure 2 - SEM micrographs of the NC matrix surface at magnifications of (a) 5 000x and (b) 20 000x; and after freeze-drying process at magnifications of (c) 2 050x and (d) 4 300x.

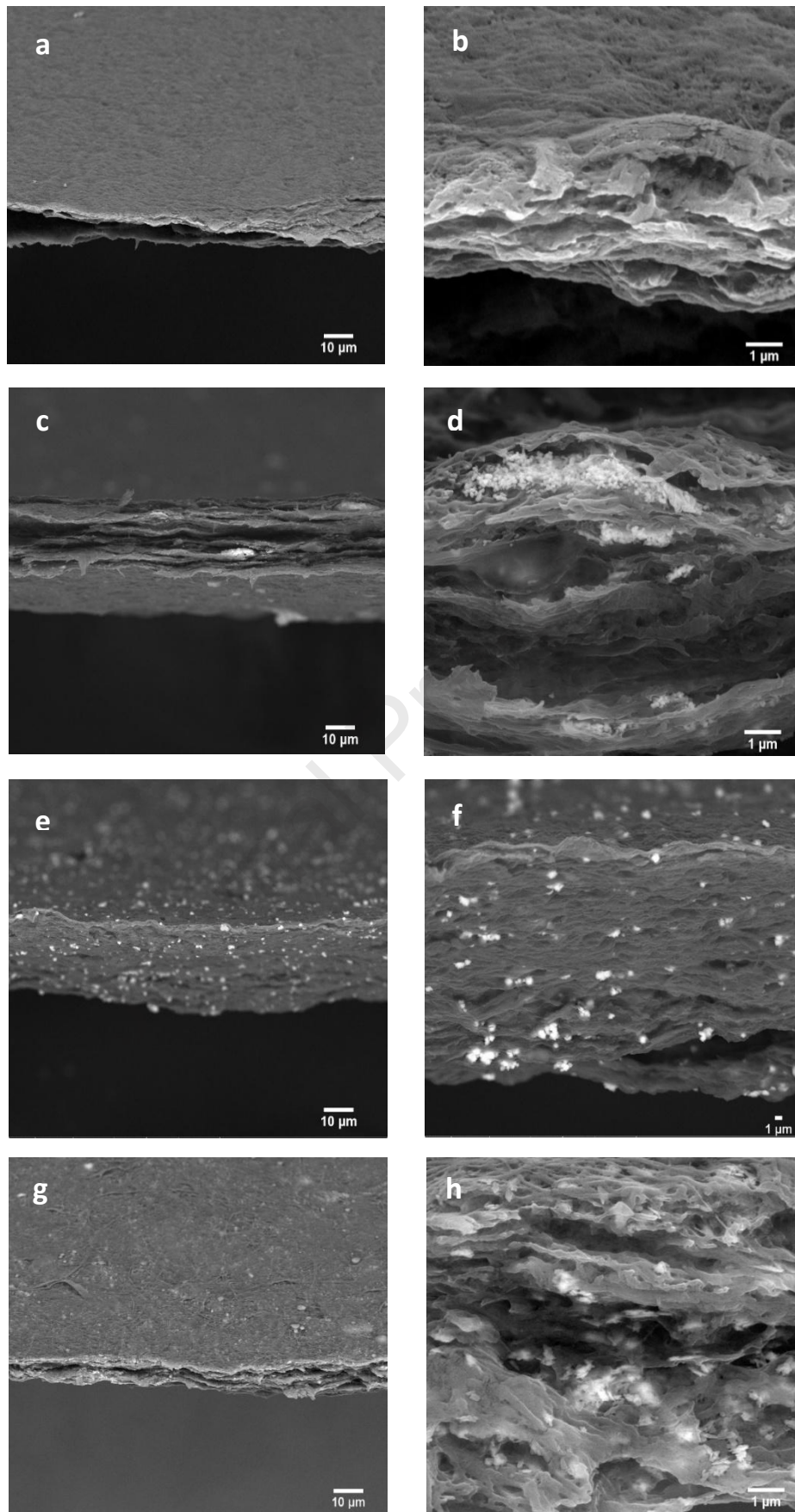


Figure 3 - Cross-section SEM micrographs of the films: NC (a, b), NC/ZnO-SP (c, d), NC/ZnO-FL (e, f), and NC/ZnO-SH (g, h). Magnifications: 2 000x (a, c, e, g); 5 000x (f); 25 000x (b, d, h).

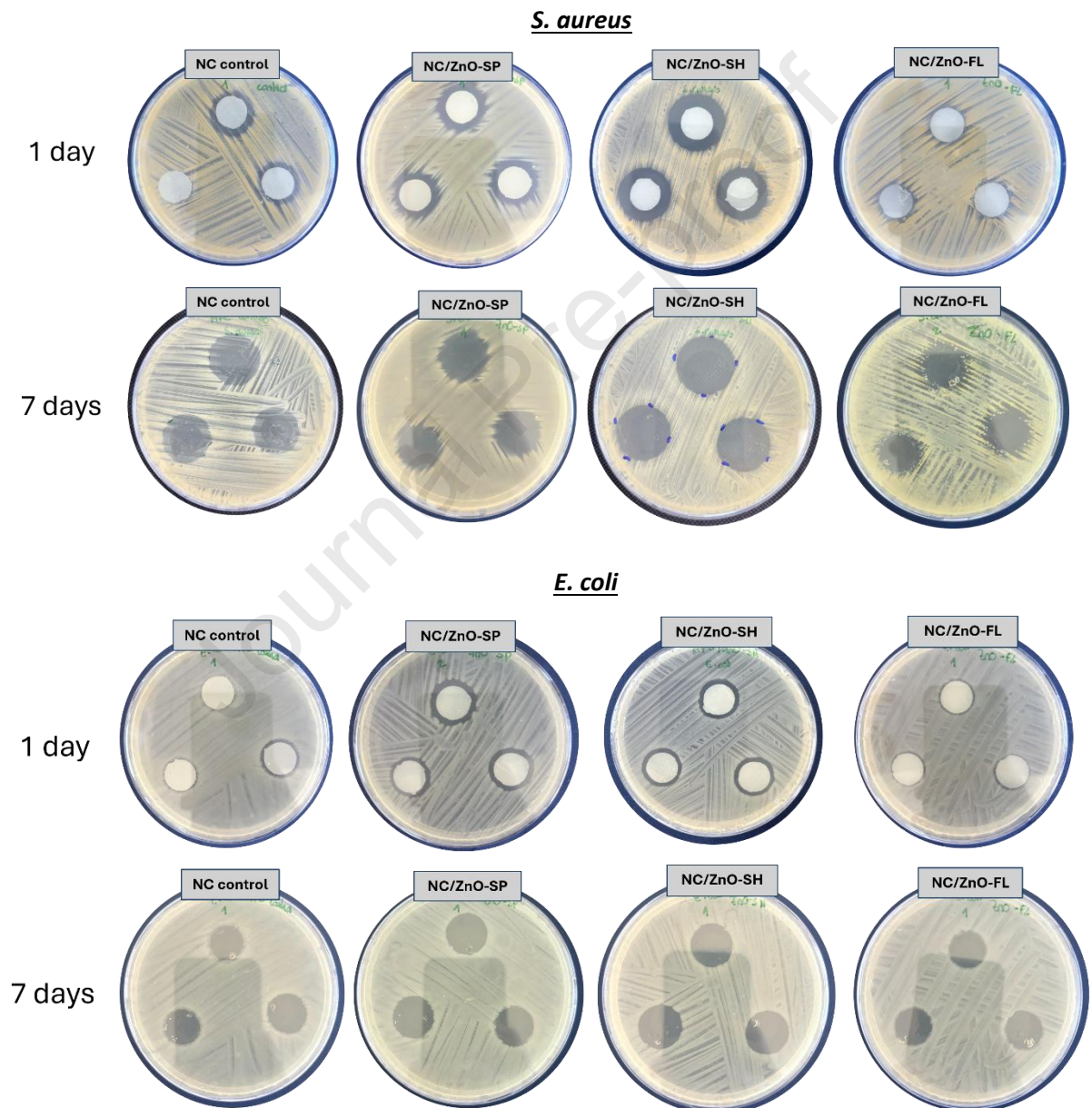


Figure 4 – Agar diffusion assay of NC/ZnO films against *S. aureus* and *E. coli* after 24 h of incubation and 7 days after disc removal.

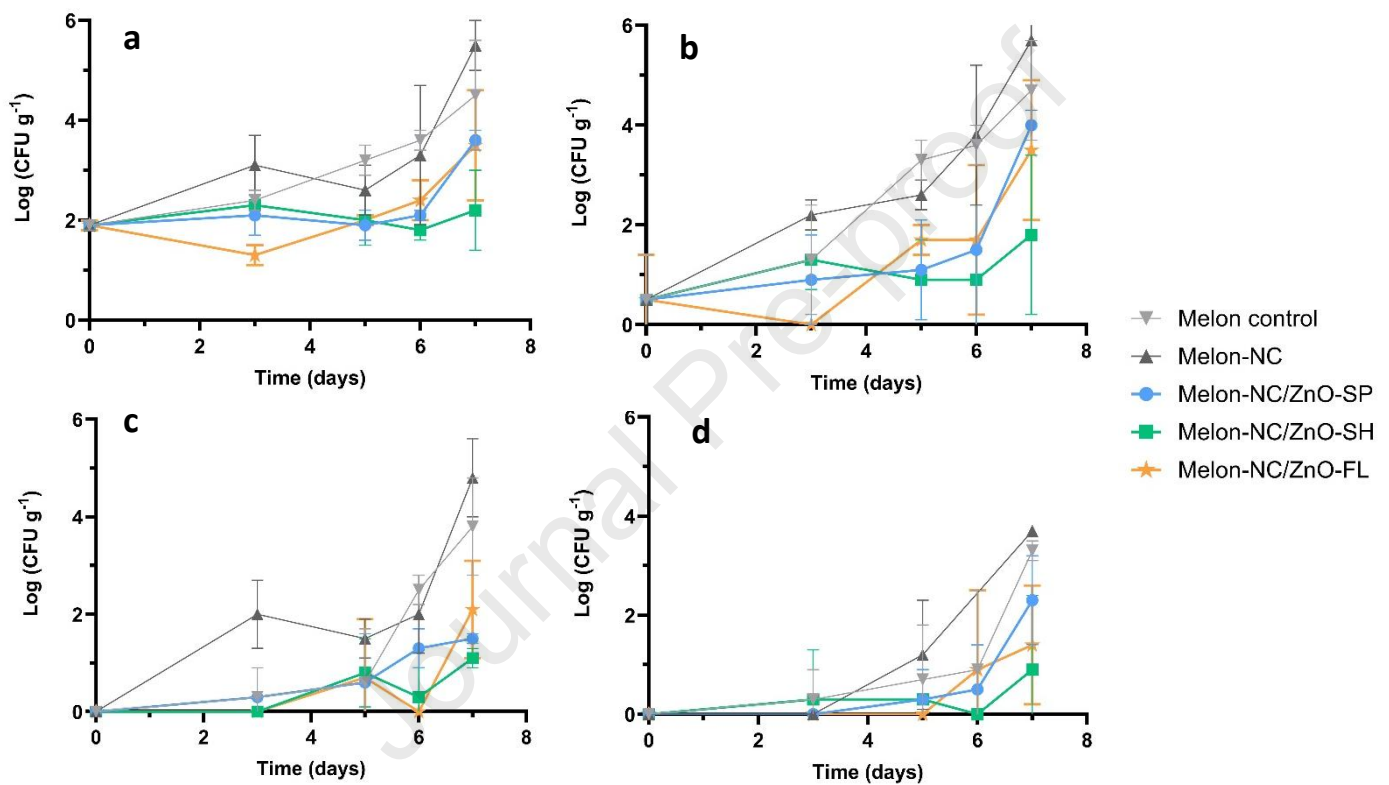


Figure 5 - Microbial counts of fresh-cut melon samples stored at 4 °C for 7 days: a) total aerobic counts at 30 °C, b) total aerobic counts at 7 °C, c) *Enterobacteriaceae*, and d) yeasts and moulds. Samples include melon control, NC film control, and NC films containing ZnO NPs (SP, SH, FL). Results are expressed as mean \pm standard deviation (n = 3) and reported as log CFU g⁻¹.

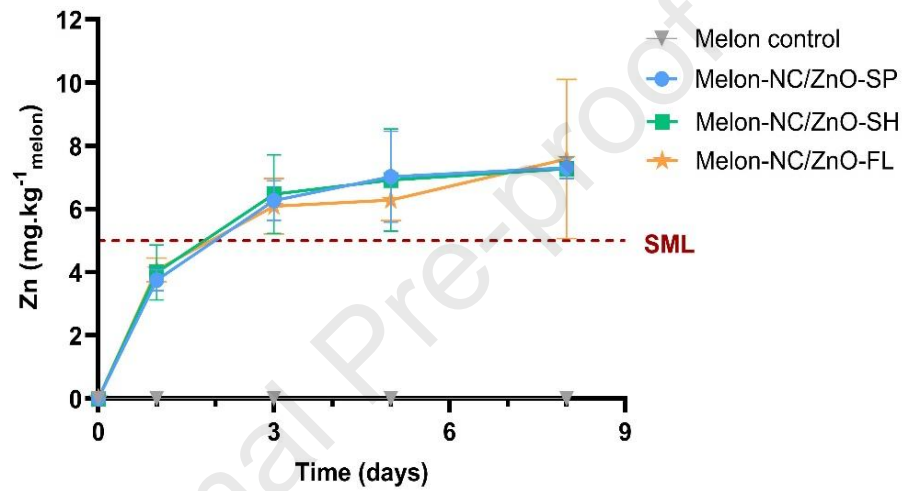


Figure 6 – Zn migration from NC/ZnO nanocomposite films into fresh-cut melon during storage at 4 °C for 8 days, under a realistic scenario ($A/M = 1 \text{ dm}^2 \text{ kg}^{-1} \text{ food}$). Results are expressed as mean \pm standard deviation ($n = 3$) and reported as mg kg^{-1} melon. The SML (5 mg kg^{-1}) food is indicated for reference.

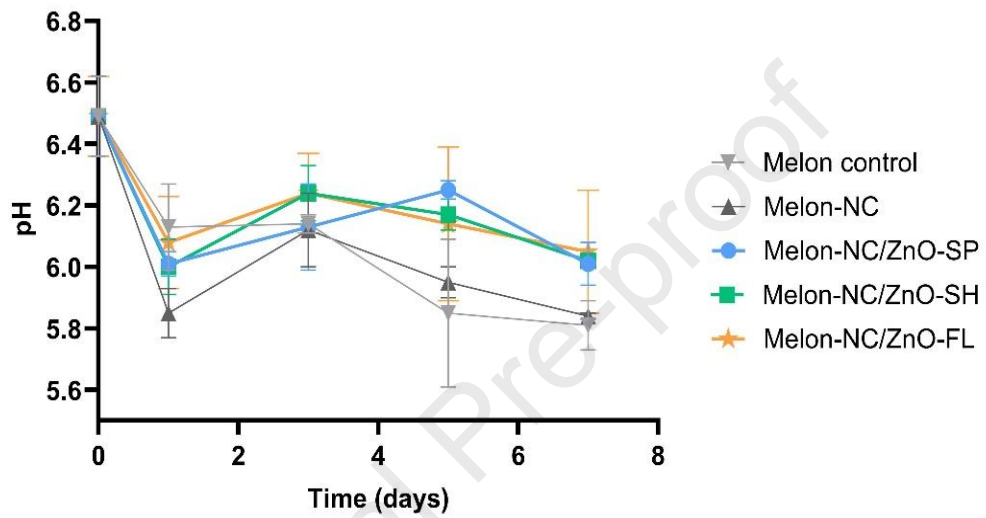


Figure 7 – Evolution of pH in fresh-cut melon samples stored at 4 °C for 7 days. Samples include melon control, NC film control, and NC films containing ZnO NPs (SP, SH, FL). Results are expressed as mean \pm standard deviation (n = 3).

Highlights

- Nanocellulose films incorporating ZnO NPs were developed for active food packaging
- NC/ZnO films reduced microbial growth on refrigerated fresh-cut melon
- Sheet-shaped ZnO showed the highest antimicrobial efficacy in melon fruit
- Zn migration reached specific migration limit by day 2 remaining stable afterwards
- NC/ZnO films maintained higher melon pH consistent with microbial growth inhibition

Journal Pre-proof

Declaration of interests

The authors declare that they have no known competing financial interests or personal relationships that could have appeared to influence the work reported in this paper.

The authors declare the following financial interests/personal relationships which may be considered as potential competing interests:

Fátima Poças
On Behalf of all authors as Correspondent author
Porto 28th January 2026

Journal Pre-proof